Electronic Supplementary Material (ESI) for ChemComm.

Supporting Information

A strongly Lewis-acidic and fluorescent borenium cation supported by a tridentate formazanate ligand

Benjamin D. Katzman, Ryan R. Maar, Daniela Cappello, Madeleine O. Sattler, Paul D. Boyle, Viktor N. Staroverov, and *Joe B. Gilroy**

Department of Chemistry and The Centre for Advanced Materials and Biomaterials Research (CAMBR), The University of Western Ontario, 1151 Richmond St. N., London, Ontario, N6A 5B7, Canada. E-mail: joe.gilroy@uwo.ca.

Table of Contents

EXPERIMENTAL TECHNIQUES

General Considerations

Reactions and manipulations were carried out under an N_2 atmosphere using standard glove box or Schlenk techniques unless otherwise stated. Reagents were purchased from Sigma-Aldrich, Alfa Aesar, Oakwood Chemicals, or Strem Chemicals and used as received unless otherwise noted. $[Et_3Si(C_7H_8)][B(C_6F_5)_4]$[1] and $[nBu_4N][B(C_6F_5)_4]$[2] were prepared according to published procedures. $[Et_3Si(C_7H_8)][B(C_6F_5)_4]$ was used immediately upon isolation and gave better results than silylium reagents that were not stabilized by toluene coordination. Solvents were purchased from Caledon Laboratories, dried using an Innovative Technologies Inc. solvent purification system, collected under vacuum, and stored under an N_2 atmosphere over 4 Å molecular sieves. Toluene used for the synthesis of $\mathbf{9}^+$ was further stirred over and distilled from CaH_2 and stored over 4 Å molecular sieves before use. CH_2Cl_2 used for cyclic voltammetry and UV-vis absorption and emission spectroscopy of $\mathbf{9}^+$ was passed through a silica (oven dried at 180 °C for 72 h) packed column, stirred over and distilled from CaH_2, and then stirred and distilled from $AlCl_3$ twice before being stored over 4 Å molecular sieves for 48 h before use. NMR spectra were recorded at 25 °C on a 400 MHz (^{1}H: 399.8 MHz; ^{11}B{^{1}H}: 128.3 MHz; ^{13}C{^{1}H}: 100.5 MHz; ^{19}F{^{1}H}: 376.1 MHz, ^{31}P{^{1}H}: 161.9 MHz) Varian INOVA spectrometer at 25 °C. ^{1}H NMR spectra were referenced to residual $CHCl_3$ (δ = 7.26) or $CHDCl_2$ (δ = 5.32) or DMSO-d_5 (δ = 2.50), ^{11}B{^{1}H} spectra were referenced to BF_3•OEt_2 (δ = 0), ^{13}C{^{1}H} NMR spectra were referenced to $CDCl_3$ (δ = 77.2) or CD_2Cl_2 (δ = 54.0) or DMSO-d_6 (δ = 39.5), ^{19}F{^{1}H} NMR spectra were referenced to $CFCl_3$ (δ = 0) and ^{31}P{^{1}H} NMR spectra were referenced to H_3PO_4 (δ = 0). Mass-spectrometry data were recorded in positive or negative ion mode using a Bruker microTOF II electrospray ionization spectrometer. FT-IR spectra were recorded on a PerkinElmer Spectrum Two instrument using an attenuated total reflectance accessory. UV-vis absorption spectra were recorded on a Cary 5000 UV-Vis-NIR spectrophotometer. Molar extinction coefficients were determined from the slope of a plot of absorbance against concentration using four solutions with various known concentrations. Emission spectra were obtained using a Photon Technology International (PTI) QM-4 SE spectrofluorometer. Excitation wavelengths were chosen based on λ_{max} from the respective UV-Vis absorption spectrum of each compound in the same solvent. Absolute emission quantum yields were measured using a Hamamatsu C11347-11 Quantaurus Absolute PL Quantum Yield Spectrometer.

Gutmann-Beckett Acceptor Number Determination and Competition Experiment[3-4]

Borenium cation $\mathbf{9}^+$ or $B(C_6F_5)_3$ were combined with $OPEt_3$ in a 1:1 ratio in CD_2Cl_2. $^{31}P\{^1H\}$ NMR spectra were collected to obtain the chemical shift of the $\mathbf{9}^+\bullet OPEt_3$ (86.7 ppm) and $B(C_6F_5)_3\bullet OPEt_3$ (77.1 ppm) adducts. The obtained chemical shifts were used to compute Gutmann-Beckett acceptor numbers (ANs) using the following equation:

$$AN = 2.21 \times (\delta^{31}_{LA\cdot Et3PO} - 41)$$

For the competition experiment, borenium cation $\mathbf{9}^+$ and $B(C_6F_5)_3$ were combined in CD_2Cl_2 before $OPEt_3$ was added. The ratio of the three species was 1:1:0.95 (deficient in $OPEt_3$). The $\mathbf{9}^+\bullet OPEt_3$:$B(C_6F_5)_3\bullet OPEt_3$ ratio, determined by integration of the respective $^{31}P\{^1H\}$NMR signals, was 1:0.8.

Elemental Analysis

Data were recorded using an Elementar Vario EL Cube (VarioElcube Software v4.0.13) instrument operated at 1150 °C under Ar in CHNS mode. Samples were prepared in an MBraun Glovebox and sulfur levels were either below the detection limit (<0.2%) or not detected.

Cyclic Voltammetry

Cyclic voltammetry experiments were performed in an Ar filled glovebox, using a Bioanalytical Systems Inc. (BASi) Epsilon potentiostat and analyzed using BASi Epsilon software. Typical electrochemical cells consisted of a three-electrode setup including a silver *pseudo*-reference electrode, glassy carbon working electrode, and platinum counter electrode. Experiments were run at a scan rate of 250 mV s^{-1} in CH_2Cl_2 solutions of the analyte (~1 mM) and supporting electrolyte (0.1 M $[n Bu_4N][B(C_6F_5)_4]$). Cyclic voltammograms were referenced relative to the ferrocene/ferrocenium (Fc/Fc^+) redox couples (~1 mM internal standard) and corrected for internal cell resistance using the BASi Epsilon software. Borenium cation $\mathbf{9}^+$ reacts with ferrocene. To circumvent this issue, 1,1'-dibromoferrocene was added as an internal reference for $\mathbf{9}^+$. A scan of a 1:1 solution of ferrocene:1,1'-dibromoferrocene under identical conditions was then collected to determine the oxidation potential of 1,1'-dibromoferrocene (0.33 V) relative to Fc/Fc^+. This value was then used to reference the voltammogram of $\mathbf{9}^+$ to the Fc/Fc^+ redox couple.

X-RAY DIFFRACTION DATA AND METHODS

Data Collection and Processing

Single crystals suitable for X-ray diffraction studies were grown by layering a THF solution with *n*-pentane and cooling at –20 °C (**8**) or by slowly cooling a saturated toluene solution at –20 °C (**9**$^+$). The samples were mounted on MiTeGen polyimide micromounts with a small amount of Paratone *N* oil. X-ray diffraction measurements were made on a Bruker Kappa Axis Apex2 or Bruker-Nonius KappaCCD Apex2 diffractometer at a temperature of 110 K. The data collection strategy involved a number of ω and φ scans, which collected data up to 134.74° (2θ, **8**) and 47.124° (2θ, **9**$^+$). The frame integration was performed using SAINT.[5] The resulting raw data was scaled and absorption corrected using a multi-scan averaging of symmetry equivalent data using SADABS.[6]

Structure Solution and Refinement

The structures were solved by using a dual space methodology using the SHELXT program.[7] All non-hydrogen atoms were obtained from the initial solution for **8**. The hydrogen atoms were introduced at idealized positions and were allowed to refine isotropically. For **9**$^+$, most non-hydrogen atoms were obtained from the initial solution. The remaining atoms were recovered from a difference Fourier map. All the hydrogen atoms on the cation (**9**$^+$) except those bound to C20 were introduced at idealized positions and were allowed to refine isotropically. The structural models were fit to the data using full matrix least-squares based on F^2. The calculated structure factors included corrections for anomalous dispersion from the usual tabulation. The structures were refined using the SHELXL program from the SHELX suite of crystallographic software.[8] The Mercury v3.10.3 software package was used to generate graphical representations of the solid-state structures. See Tables S1 and S2 and CCDC 2091368 and 2091369 for additional crystallographic data.

Treatment of Disorders

For **8**:

A difference Fourier map showed that the hydrogen atom positions for methyl group (C20) were disordered over two orientations. This disorder was modelled by assuming an idealized disordered

methyl group and fixing the occupancy at 50:50 for the two orientations.

For **9**$^{+}$:

The hydrogen atoms bound to methyl group C20 were disordered and were modelled as a second conformation where the hydrogen atom positions were rotated 60º relative to the other set of hydrogen atom positions. The occupancies were allowed to refine and converged to value of 0.50(3). For the final refinement cycles, the occupancy for the methyl disorder was fixed at 0.5000. In addition, the asymmetric unit contains two sites of disordered toluene molecules – one on a general position and the other was in the vicinity of a crystallographic centre of symmetry. The disordered toluene near the centre of symmetry could not be reasonably modelled and was subjected to the SQUEEZE procedure as implemented by the PLATON program.[9] The disordered toluene molecule residing at a general position in the unit cell was modelled using a conventional split atom refinement. The centroids of the aromatic rings differed by 0.49 Å. The methyl groups were rotated by roughly 172º relative to one another. The angle between the two sets of ring atoms was 2.4º.

Table S1 X-ray diffraction data collection and refinement details for boron formazanate **8** and **9**$^{+}$.

	8	**9**$^{+}$
Formula	$C_{21}H_{18}BFN_4O$	$C_{52}H_{26}B_2F_{20}N_4O$
FW (g mol^{-1})	372.20	1124.39
Crystal Habit	Purple Prism	Purple Plate
Crystal System	Monoclinic	Monoclinic
Space Group	$P2_1/c$	$P2_1/c$
T (K)	110	110
λ (Å)	1.54178	0.71073
a (Å)	9.0367(10)	17.113(6)
b (Å)	13.9481(14)	20.345(7)
c (Å)	14.746(2)	15.711(6)
α (°)	90	90
β (°)	105.215(5)	115.728(10)
γ (°)	90	90
V (Å^3)	1793.5(4)	4928(3)
Z	4	4
ρ (g cm^{-3})	1.378	1.516
μ (cm^{-1})	0.766	0.144
R_1,[a] ωR_2[b][I > 2σ]	0.0333, 0.0848	0.0302, 0.0703
R_1, ωR_2 (all data)	0.0360, 0.0867	0.0478, 0.0785
GOF[c]	1.029	1.018

Where:
[a] $R_1 = \Sigma(|F_o|-|F_c|)/\Sigma F_o$
[b] $\omega R_2 = [\Sigma(\omega(F_o^2-F_c^2)^2)/\Sigma(\omega F_o^4)]^{½}$
[c] $GOF = [\Sigma(\omega(F_o^2-F_c^2)^2)/(\text{No. of reflns.}-\text{No. of params.})]^{½}$

Table S2 Selected bond lengths (Å), bond angles (°), and structural metrics extracted from the solid-state structures of boron formazanates **8** and $\mathbf{9}^{+}$.

	8	$\mathbf{9}^{+}$
N1-N2	1.3115(14)	1.334(2)
N3-N4	1.3123(14)	1.319(2)
N2-C1	1.3499(16)	1.339(2)
N3-C1	1.3372(16)	1.339(2)
B1-N1	1.5827(17)	1.460(3)
B1-N4	1.5525(17)	1.451(3)
B1-F1	1.3933(16)	–
B1-O1	1.4043(17)	1.333(3)
N1-B1-N4	99.48(10)	113.09(17)
N1-B1-O1	117.48(11)	124.44(18)
N4-B1-O1	112.70(11)	122.41(19)
N2-N1-B1	119.28(10)	121.11(16)
N3-N4-B1	121.52(10)	123.98(16)
N2-C1-N3	124.17(11)	126.37(17)
F1-B1-O1	110.59(11)	–
C9-C21-O1	111.80(11)	113.98(16)
C21-O1-B1	117.68(10)	122.06(16)
Dihedral angles[a]	20.58(6), 42.29(5)	11.03(13), 25.75(11)
Boron displacement[b]	0.6190(19)	0.056(3)

[a]Defined as the angle between the *N*-aryl substituents and the N_4 (N1-N2-N3-N4) plane of the formazanate ligand backbone. [b]Defined as the distance between B1 and the N_4 (N1-N2-N3-N4) plane of the formazanate ligand backbone.

SYNTHETIC PROCEDURES

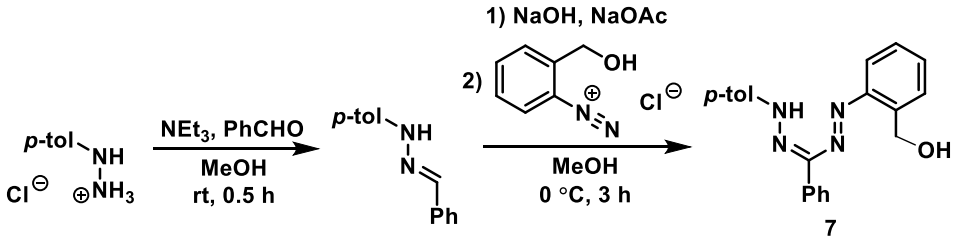

Scheme S1 Synthesis of formazan **7**.

Formazan 7

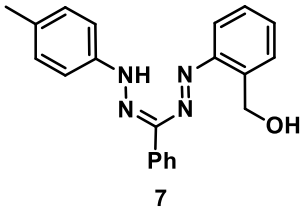

In air, *p*-tolylphenylhydrazine hydrochloride (3.96 g, 25.0 mmol) was suspended in MeOH (75 mL) and stirred for 10 min before NEt_3 (4.50 g, 6.20 mL, 44.4 mmol) was added. The solution was stirred for 15 min before benzaldehyde (2.9 g, 27 mmol) was added dropwise. The pale-yellow solution was stirred for 1 h. MeOH (150 mL) was added and the mixture was treated with NaOH (4.00 g, 100 mmol) and NaOAc (5.79 g, 70.6 mmol). The resulting orange hydrazone-containing solution was cooled to 0 °C for 30 min. In a separate flask, 2-aminobenzyl alcohol (3.76 g, 30.5 mmol) was dissolved in H_2O (40 mL) and concentrated hydrochloric acid (9.0 mL, 1.1×10^2 mmol) was added dropwise before the flask was cooled to 0 °C. A solution of sodium nitrite (2.42 g, 35.1 mmol) was dissolved in H_2O (15 mL), cooled to 0 °C, and added dropwise to the 2-aminobenzyl alcohol solution. This diazonium salt containing solution was stirred for 10 min and then added dropwise to the orange hydrazone-containing solution. The reaction mixture turned dark red immediately upon addition of the diazonium salt, and was stirred for 3 h at 0 °C. During this time, large quantities of solid **7** precipitated from solution. The reaction mixture was neutralized with 1 M HCl (*ca.* 60 mL) and the resulting dark red precipitate was collected and washed with MeOH. The crude solid was purified using column chromatography (silica gel, CH_2Cl_2), before the volatiles were removed *in vacuo* and the resulting residue was triturated with MeOH to afford formazan **7** as a fluffy red solid. Yield = 3.81 g, 43%. M.p.: 183–185 °C. ^{1}H NMR (399.8 MHz, DMSO-d_6): δ 14.95 (s, 1H, N*H*), 8.11 (d, $^3J_{HH}$ = 7 Hz, 2H, aryl C*H*), 7.99–7.95 (m, 3H, aryl C*H*), 7.48 (t, $^3J_{HH}$ = 8 Hz, 2H, aryl C*H*), 7.44–7.34 (m, 5H,

aryl C*H*), 7.14 (t, $^{3}J_{HH}$ = 8 Hz, 1H, aryl C*H*), 5.65 (t, $^{3}J_{HH}$ = 6 Hz, 1H, O*H*), 4.68 (d, $^{3}J_{HH}$ = 6 Hz, 2H, CH_2), 2.40 (s, 3H, CH_3). $^{13}C\{^{1}H\}$ NMR (100.5 MHz, DMSO-d_6): δ 148.9, 143.3, 141.0, 140.6, 136.9, 130.2, 130.1, 129.0, 128.9, 128.6, 127.7, 125.6, 124.5, 121.0, 114.3, 61.7, 21.1. FT-IR (ATR): 3329 (b), 3181 (w), 3022 (w), 1518 (m), 1230 (m), 1003 (s), 821 (s), 757 (s), 668 (s), 629 (s) cm^{-1}. UV-vis (CH_2Cl_2): λ_{max} 484 nm (ε = 17,800 M^{-1} cm^{-1}), 305 nm (ε = 26,400 M^{-1} cm^{-1}). Mass Spec. (ESI, –ve mode): exact mass calculated for $[C_{21}H_{19}N_4O]^-$, [M–H]$^-$: 343.1559; exact mass found: 343.1569; difference: +2.9 ppm. Anal. Calcd. (%) for $C_{21}H_{20}N_4O$: C, 73.23; H, 5.85; N, 16.27. Found: C, 73.38; H, 6.35; N, 16.75.

BF Formazanate 8

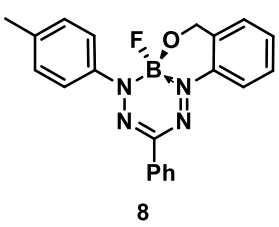

8

Formazan **7** (0.501 g. 1.45 mmol) was dissolved in dry toluene (80 mL). NEt_3 (0.47 g, 0.65 mL, 4.6 mmol) was added and the solution was stirred for 10 min. BF_3•OEt_2 (1.24 g, 1.10 mL, 8.80 mmol) was then slowly added and the solution was heated at 120 °C for 48 h. The solution gradually turned from red to magenta during this time. The solution was cooled to 21 °C and deionized H_2O (15 mL) was added to quench any excess reactive boron-containing species. The solution was transferred to a seperatory funnel and washed with deionized H_2O (3 × 100 mL), dried over $MgSO_4$, gravity filtered and concentrated *in vacuo* to afford the crude BF formazanate **8**. The product was purified using column chromatography (silica gel, toluene). The resulting magenta solution was concentrated *in vacuo* and the solids were washed with *n*-pentane to afford BF formazanate **8** as a dark purple solid (green reflex). Yield = 0.327 g, 61%. M.p.: 208–210 °C. ^{1}H NMR (399.8 MHz, $CDCl_3$): δ 8.19 (d, $^{3}J_{HH}$ = 8 Hz, 1H, aryl C*H*), 8.15 (d, $^{3}J_{HH}$ = 7 Hz, 2H, aryl C*H*), 7.91 (d, $^{3}J_{HH}$ = 9 Hz, 2H, aryl C*H*), 7.51–7.42 (m, 3H, aryl C*H*), 7.38 (t, $^{3}J_{HH}$ = 7 Hz, 1H, aryl C*H*), 7.31–7.28 (m, 2H, aryl C*H*), 7.13 (d, $^{3}J_{HH}$ = 8 Hz, 1H, aryl C*H*), 5.27 (d, $^{2}J_{HH}$ = 15 Hz, 1H, diastereotopic CH_2), 4.82 (d, $^{2}J_{HH}$ = 15 Hz, 1H, diastereotopic CH_2), 2.42 (s, 3H, CH_3). $^{11}B\{^{1}H\}$ NMR (128 MHz, $CDCl_3$): δ –0.8 (d, $^{1}J_{BF}$ = 38 Hz). $^{13}C\{^{1}H\}$ NMR (100.5 MHz, $CDCl_3$): δ 150.0, 141.9, 140.5, 140.1, 133.9, 132.5, 129.8, 129.4, 128.9, 128.8, 128.7, 125.8, 125.7, 123.9, 118.4, 62.4, 21.5. $^{19}F\{^{1}H\}$ NMR (376.1 MHz, $CDCl_3$): δ –156.1 (q, $^{1}J_{FB}$ = 38 Hz). FT-IR (ATR): 3024 (w), 2959 (w), 1602 (m), 1487 (m), 1457 (m), 1377 (m), 1353 (s), 1276 (s), 1234 (s), 1165 (m), 1068 (m), 981 (s), 923 (s), 877 (s), 791 (w), 763 (s), 696 (s), 666 (s), 572 (s), 540 (s) cm^{-1}. UV-vis (CH_2Cl_2): λ_{max} 530 nm (ε = 20,200 M^{-1} cm^{-1}), 355 nm (ε =

6,400 M^{-1} cm^{-1}), 316 nm (ε = 22,400 M^{-1} cm^{-1}). Mass Spec. (ESI, –ve mode): exact mass calculated for $[C_{21}H_{18}N_4OBF]^-$, $[M]^-$: 372.1558; exact mass found: 372.1558; difference: 0.0 ppm. Anal. Calcd. (%) for $C_{21}H_{18}N_4OBF$: C, 67.77; H, 4.87; N, 15.05. Found: C, 67.54; H, 5.17; N, 15.25.

Borenium cation 9^+

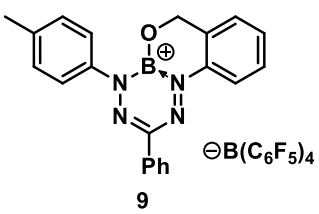

9

Freshly prepared $[Et_3Si(C_7H_8)][B(C_6F_5)_4]$ (0.098 g 0.11 mmol) was dissolved in toluene (2 mL) and stirred for 5 min. In a separate vial, BF formazanate **8** (0.041 g, 0.11 mmol) was dissolved in toluene (5 mL) and stirred for 5 min. The magenta BF formazanate **8** solution was added dropwise to the triethylsilylium cation solution over a 5 min period. During the addition, the colour changed from magenta to teal. The teal solution was stirred at 21 °C for 1 h before it was concentrated *in vacuo*. The resulting solid was suspended in *n*-pentane (10 mL) and stirred for 15 min. The suspension was filtered and further washed with *n*-pentane (3 × 5 mL) to afford cation $\mathbf{9}^+$ as a shiny, dark green microcrystalline solid. Yield = 0.098 g, 87%. M.p.: 218–220 °C. ^{1}H NMR (399.8 MHz, CD_2Cl_2): δ 8.48 (d, $^3J_{HH}$ = 9 Hz, 1H, aryl C*H*), 8.29 (d, $^3J_{HH}$ = 8 Hz, 2H, aryl C*H*), 8.10 (d, $^3J_{HH}$ = 9 Hz, 2H, aryl C*H*), 7.76 (t, $^3J_{HH}$ = 8 Hz, 1H, aryl C*H*), 7.70–7.62 (m, 4H, aryl C*H*), 7.51 (d, $^3J_{HH}$ = 8.7 Hz, 2H, aryl C*H*), 7.36 (d, $^3J_{HH}$ = 8 Hz, 1H, aryl C*H*), 5.86 (s, 2H, CH_2), 2.54 (s, 3H, CH_3). ^{11}B{^{1}H} NMR (128.3 MHz, CD_2Cl_2): δ 21.2 (br s), –16.8 (s). ^{13}C{^{1}H} NMR (101 MHz, CD_2Cl_2): δ 156.3, 149.9, 147.6, 141.2, 140.0, 138.1, 137.2, 136.2, 135.6, 133.2, 132.0, 131.9, 130.9, 130.3, 130.1, 127.6, 127.2, 124.2, 119.2, 67.6, 22.2. ^{19}F{^{1}H} NMR (376.1 MHz, CD_2Cl_2): δ –133.2 (s), –163.7 (t, $^3J_{FF}$ = 20 Hz), –166.63 – –167.7 (m). FT-IR (ATR): 3032 (w), 1645 (m), 1593 (m), 1511 (m), 1457 (s), 1389 (m), 1273 (m), 1123 (m), 1082 (s), 975 (s), 828 (m), 774 (s), 755 (m), 682 (m), 660 (s), 572 (m) cm^{-1}. UV-vis (CH_2Cl_2): λ_{max} 650 nm (ε = 8,000 M^{-1} cm^{-1}), 605 nm (ε = 7,100 M^{-1} cm^{-1}), 427 nm (ε = 3,500 M^{-1} cm^{-1}), 309 nm (ε = 3,500 M^{-1} cm^{-1}). Mass Spec. (ESI, +ve mode): exact mass calculated for $[C_{21}H_{18}N_4OB]^+$, $[M]^+$: 353.1574; exact mass found: 353.1574; difference: 0.0 ppm. Anal. Calcd. (%) for $C_{45}H_{18}N_4OB_2F_{20}$: C, 52.36; H, 1.76; N, 5.43. Found: C, 52.56; H, 2.44; N, 5.13.

NMR SPECTRA

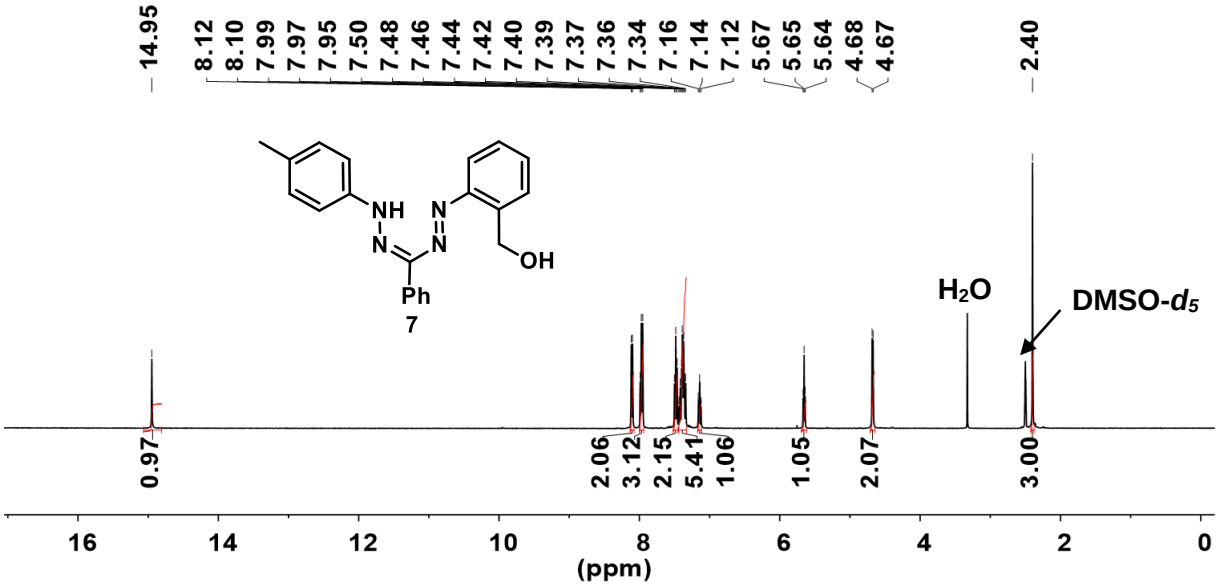

Fig. S1 ^{1}H NMR spectrum of formazan **7** recorded in DMSO-d_6.

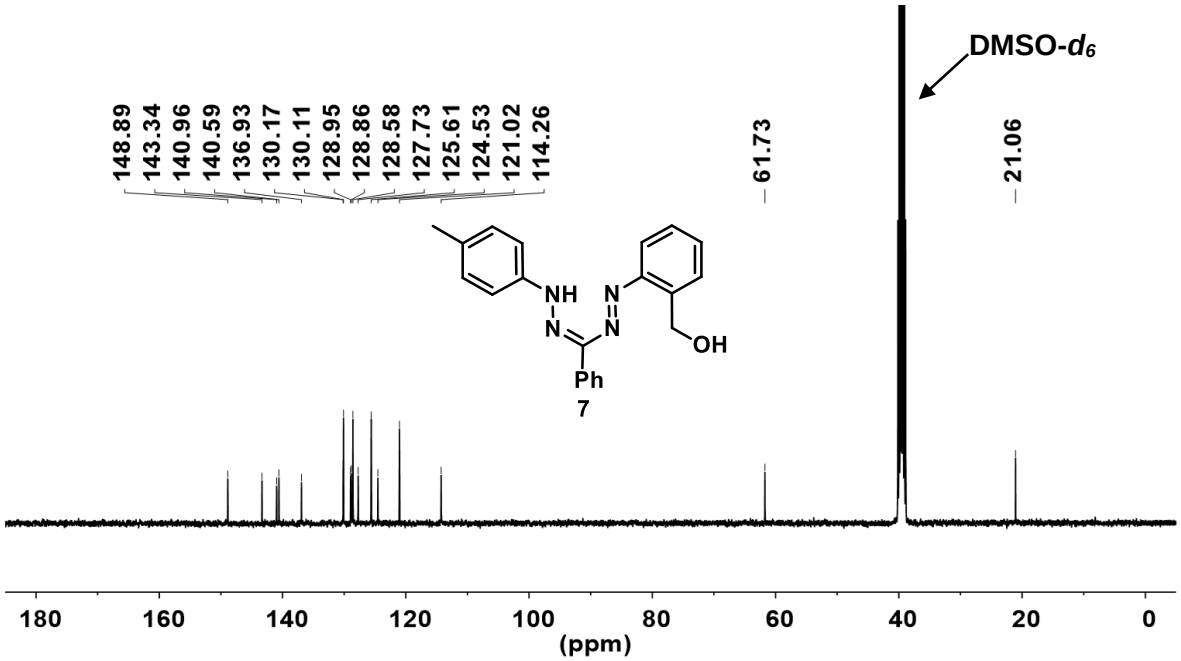

Fig. S2 ^{13}C{^{1}H} NMR spectrum of formazan **7** recorded in DMSO-d_6.

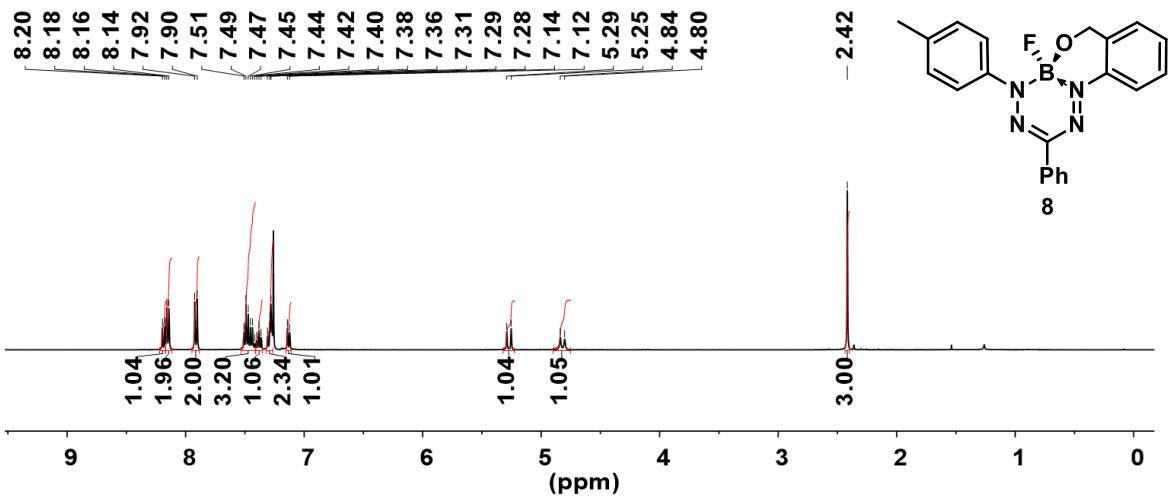

Fig. S3 ^{1}H NMR spectrum of BF formazanate **8** recorded in $CDCl_3$.

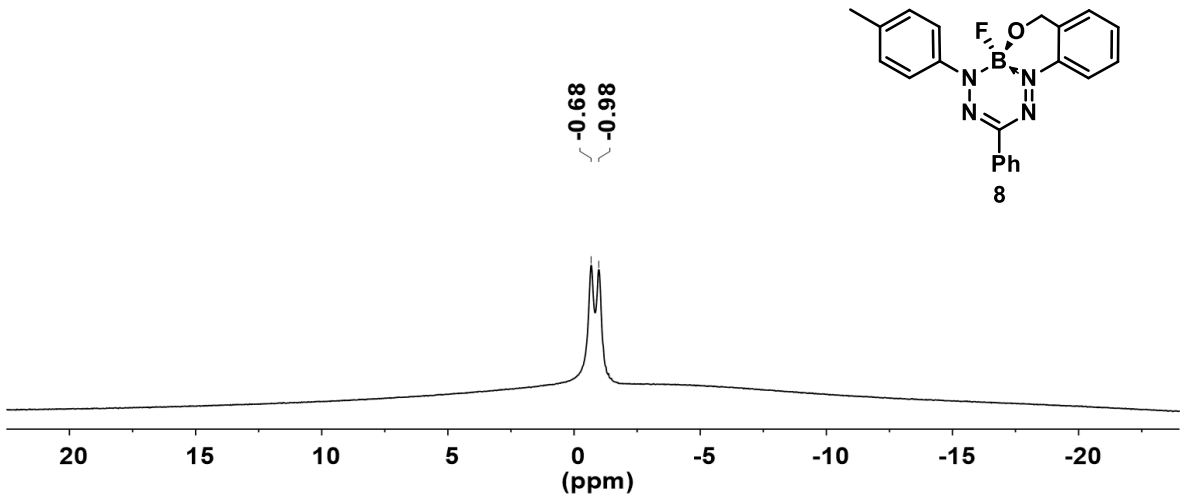

Fig. S4 ^{11}B{^{1}H} NMR spectrum of BF formazanate **8** recorded in $CDCl_3$.

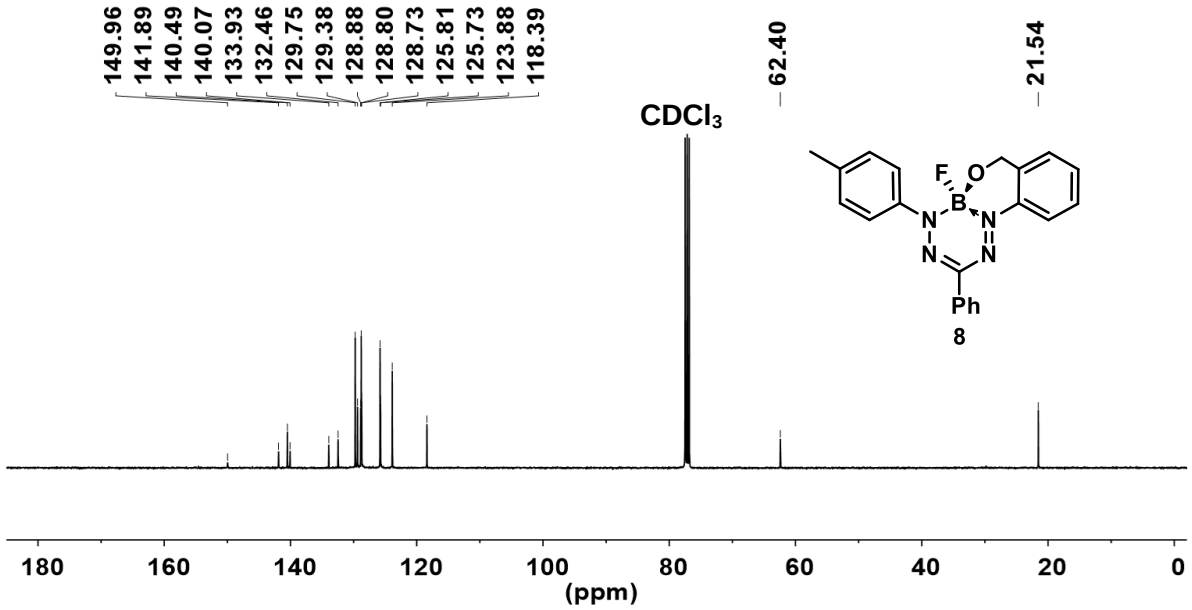

Fig. S5 $^{13}C\{^{1}H\}$ NMR spectrum of BF formazanate **8** recorded in $CDCl_3$.

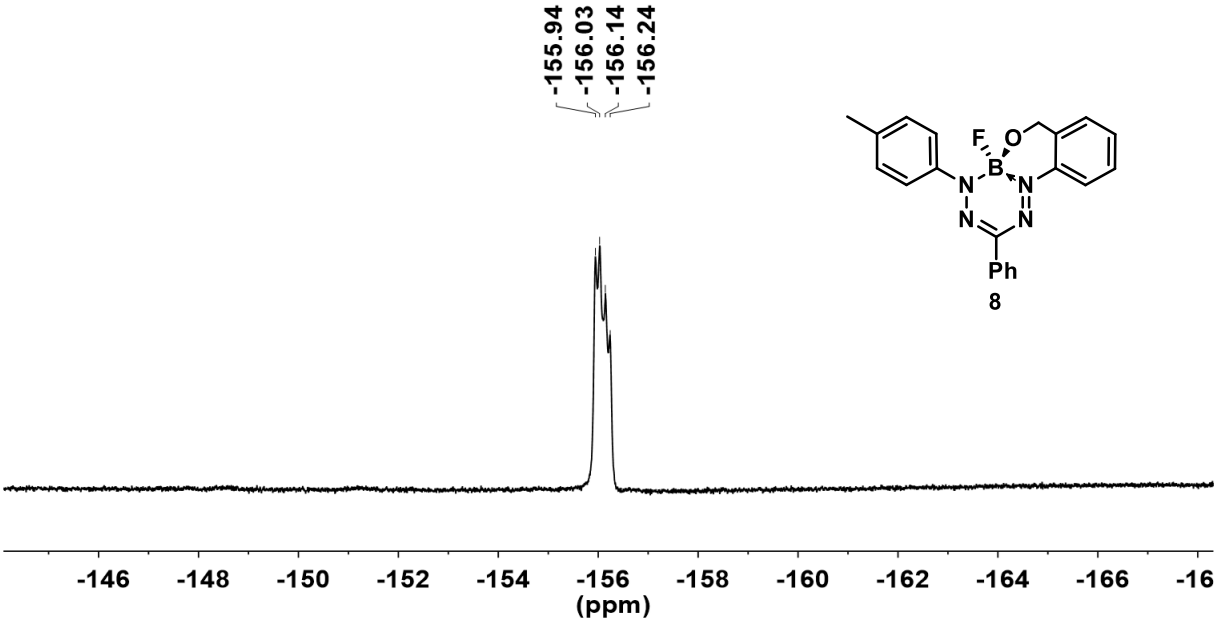

Fig. S6 $^{19}F\{^{1}H\}$ NMR spectrum of BF formazanate **8** recorded in $CDCl_3$.

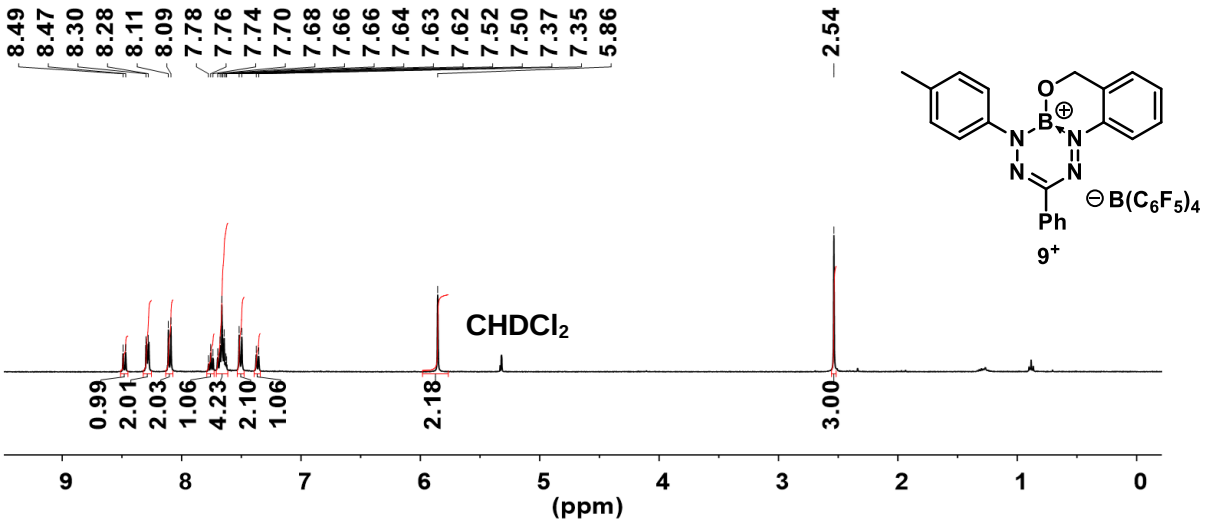

Fig. S7 ^{1}H NMR spectrum of borenium cation **9**$^{+}$ recorded in CD_2Cl_2.

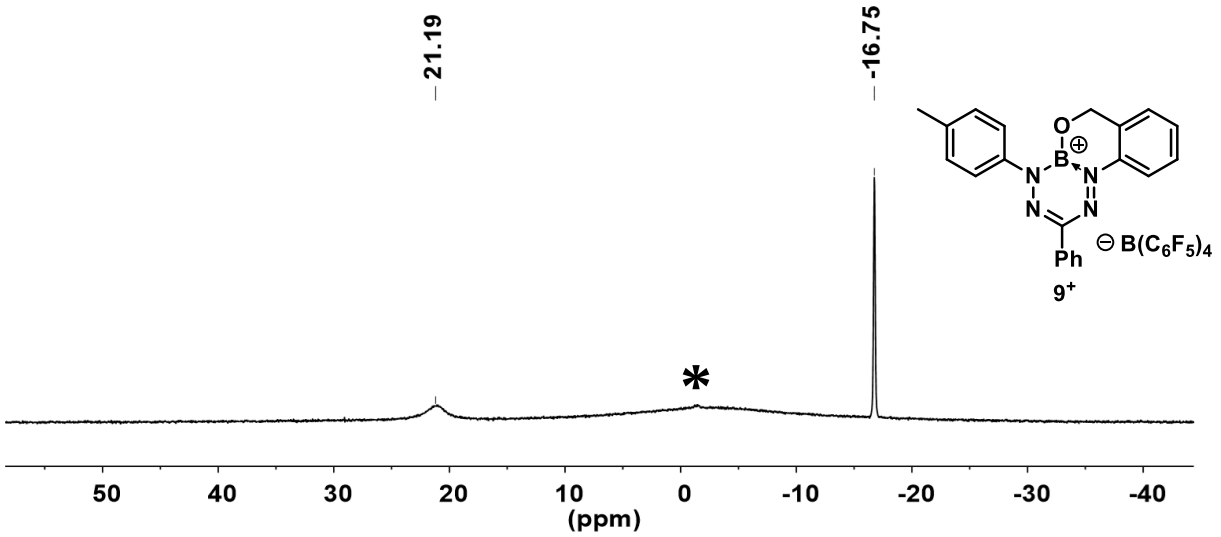

Fig. S8 ^{11}B{^{1}H} NMR spectrum of borenium cation **9**$^{+}$ recorded in CD_2Cl_2. The asterisk denotes background signal from the spectrometer probe.

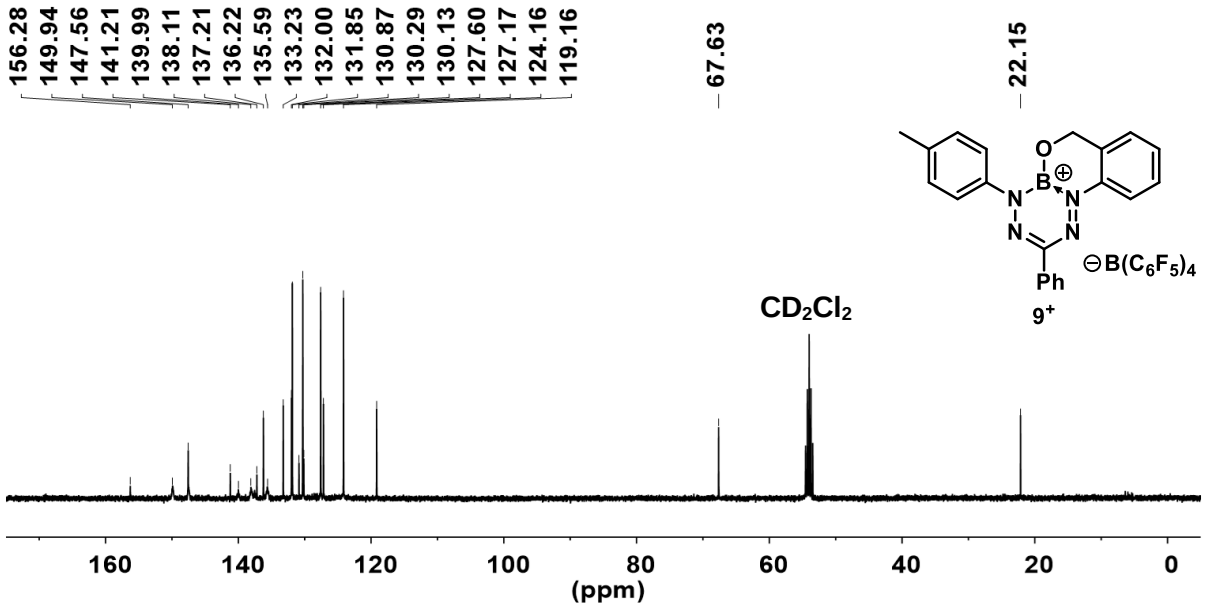

Fig. S9 $^{13}C\{^{1}H\}$ NMR spectrum of borenium cation $\mathbf{9}^{+}$ recorded in CD_2Cl_2.

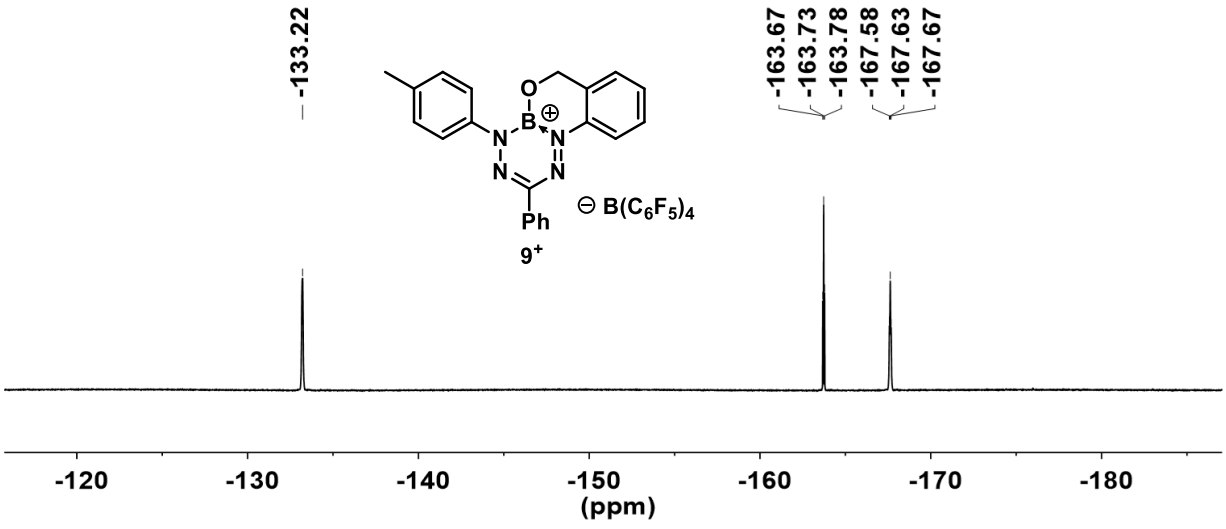

Fig. S10 $^{19}F\{^{1}H\}$ NMR spectrum of borenium cation $\mathbf{9}^{+}$ recorded in CD_2Cl_2.

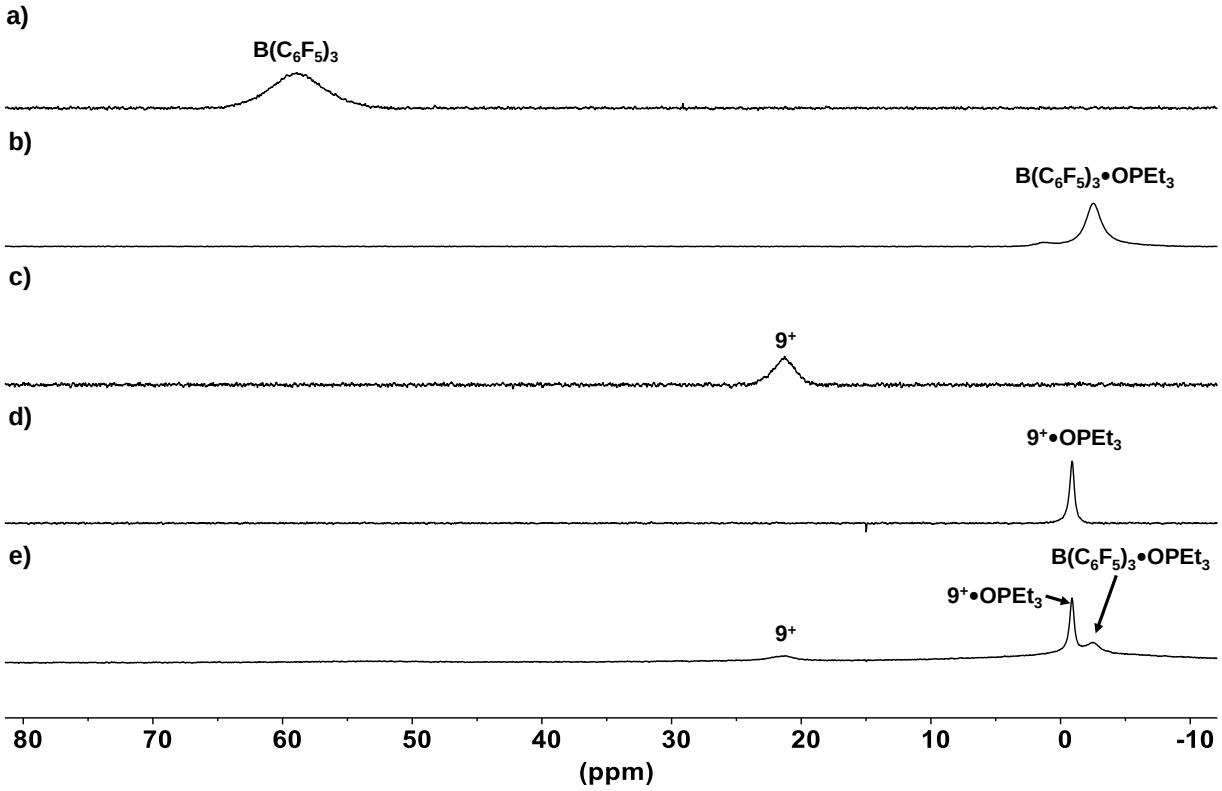

Fig. S11 $^{11}B\{^{1}H\}$ NMR spectra of CD_2Cl_2 solutions containing a) $B(C_6F_5)_3$, b) $B(C_6F_5)_3$ and $OPEt_3$, c) $\mathbf{9}^+$, d) $\mathbf{9}^+$ and $OPEt_3$, and e) $\mathbf{9}^+$, $B(C_6F_5)_3$, and $OPEt_3$ in a 1:1:0.95 ratio. The signals corresponding to $B(C_6F_5)_4^-$ (−16.8 ppm) are omitted from spectra c), d), and e) to facilitate comparison. A very broad $B(C_6F_5)_3$ signal at ~60 ppm was present in spectrum e) when the baseline was expanded.

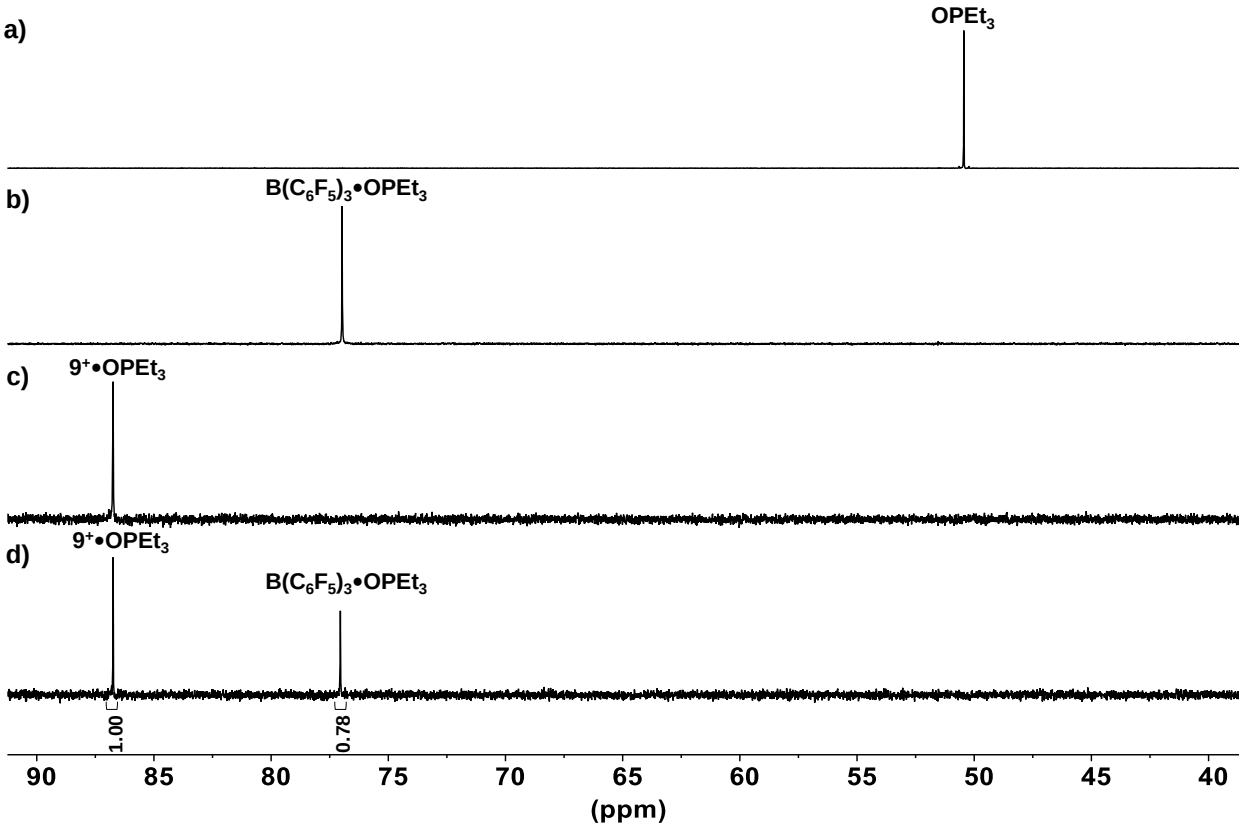

Fig. S12 $^{31}P\{^{1}H\}$ NMR spectra of CD_2Cl_2 solutions containing a) $OPEt_3$, b) $B(C_6F_5)_3$ and $OPEt_3$, c) $\mathbf{9}^+$ and $OPEt_3$, and d) $\mathbf{9}^+$, $B(C_6F_5)_3$, and $OPEt_3$ in a 1:1:0.95 ratio.

LUMO+1 OF BORENIUM CATION 9^+

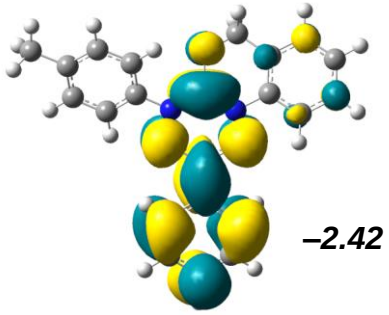

9^+

Fig. S13 LUMO+1 and its energy (in eV) calculated using the TPSSh/def2-TZVP method for borenium cation $\mathbf{9}^+$ solvated by CH_2Cl_2.

COMPUTATIONAL METHODOLOGY

All electronic structure calculations were carried out with the *Gaussian* program[10] using the TPSSh functional,[11] def2-TZVP basis set, SuperFine integration grid, and the polarizable continuum model of implicit solvation (SCRF=PCM) by CH_2Cl_2. All geometry optimizations and TDDFT calculations were performed for solvated molecules. The optimized ground-state structures were confirmed by vibrational analysis to be minima on the potential energy surface. The electronic excitation calculations were performed using non-equilibrium solvation, which is the default for single-point TDDFT runs.

OPTIMIZED GEOMETRIES OF COMPOUNDS 8 AND 9^+

Method: TPSSh/def2-TZVP SCRF(PCM,Solvent=Dichloromethane)

8, ground state (S_0)

0,1

C	3.803619	-1.658092	-0.093734
C	2.452033	-2.016092	-0.014746
C	2.107575	-3.373326	-0.040710
C	3.092511	-4.346431	-0.161226
C	4.434414	-3.983102	-0.251639
C	4.784463	-2.635079	-0.214973
C	1.412665	-0.979472	0.119475
N	1.773893	0.304594	-0.017974
N	0.879526	1.197565	0.292342
C	1.084058	2.522393	-0.147197
C	-0.049052	3.347286	-0.190670
C	0.103322	4.664798	-0.610392
C	1.353075	5.151683	-0.983804
C	2.468952	4.315656	-0.939536
C	2.342036	2.998015	-0.523422
C	-1.385819	2.752842	0.162627
O	-1.281060	1.870854	1.274230
B	-0.337275	0.824350	1.192270
N	-0.790975	-0.511949	0.459450
C	-2.117509	-0.872762	0.115316
C	-3.187121	-0.399620	0.880335
C	-4.481750	-0.784456	0.557612
C	-4.745378	-1.632018	-0.522053
C	-3.658386	-2.094810	-1.275169
C	-2.359626	-1.723610	-0.968883
C	-6.153848	-2.018781	-0.882571
F	0.111805	0.445697	2.460805
N	0.127354	-1.375475	0.138329
H	-3.003105	0.249965	1.724247
H	-5.304503	-0.423463	1.165381
H	-3.835348	-2.751488	-2.120512
H	-1.527335	-2.078763	-1.562584
H	-0.765792	5.312873	-0.647095
H	1.458716	6.181867	-1.302653
H	3.443696	4.695210	-1.222393
H	3.198224	2.338494	-0.477231
H	1.065679	-3.658424	0.033104
H	2.810604	-5.393087	-0.181442
H	5.201185	-4.743959	-0.341850
H	5.826567	-2.342438	-0.276027
H	4.079200	-0.611524	-0.058068

H	-6.835765	-1.851276	-0.047449
H	-6.212003	-3.069495	-1.175659
H	-6.512490	-1.425044	-1.729986
H	-2.093058	3.538154	0.432754
H	-1.795854	2.219249	-0.707833

9^{+}, ground state (S_0)

1,1

B	-0.010889	-1.204164	0.053718
O	-0.313138	-2.500520	0.161820
N	-1.008049	-0.138689	-0.027554
N	-0.647115	1.126825	-0.038213
N	1.664494	0.559871	-0.017544
N	1.355702	-0.712850	0.020574
C	0.653388	1.438297	-0.019085
C	-2.417630	-0.362362	-0.017741
C	-2.951805	-1.515067	-0.596635
H	-2.309874	-2.250666	-1.058983
C	-4.328055	-1.692002	-0.601514
H	-4.741285	-2.580036	-1.065743
C	-5.187695	-0.751190	-0.027770
C	-4.622720	0.394725	0.552942
H	-5.267851	1.132789	1.016220
C	-3.255993	0.598950	0.557737
H	-2.827618	1.480259	1.015208
C	2.421565	-1.652747	-0.005426
C	2.102586	-3.009261	0.145639
C	3.141995	-3.935152	0.100619
H	2.916092	-4.989440	0.213759
C	4.455744	-3.523451	-0.083756
H	5.249350	-4.259655	-0.116540
C	4.753043	-2.167264	-0.233300
H	5.776071	-1.846568	-0.383946
C	3.739116	-1.227216	-0.197692
H	3.945702	-0.174058	-0.322392
C	1.001933	2.873403	-0.024611
C	0.019886	3.837827	-0.279425
H	-0.997347	3.527380	-0.479539
C	0.352436	5.186760	-0.283440
H	-0.413375	5.926072	-0.486249
C	1.662529	5.587951	-0.032632
H	1.918807	6.640901	-0.036107
C	2.642109	4.631196	0.222690
H	3.662340	4.937062	0.422022
C	2.317340	3.280355	0.226675
H	3.079204	2.539249	0.430312

C	-6.675703	-0.954360	-0.025784
H	-6.946694	-1.908924	-0.476993
H	-7.174048	-0.155039	-0.582154
H	-7.068897	-0.928033	0.994232
C	0.700734	-3.497295	0.393637
H	0.466848	-4.335830	-0.262804
H	0.588090	-3.829171	1.428935

REFERENCES

1 S. J. Connelly, W. Kaminsky and D. M. Heinekey, *Organometallics*, 2013, **32**, 7478–7481.

2 R. J. LeSuer, C. Buttolph and W. E. Geiger, *Anal. Chem.*, 2004, **76**, 6395–6401.

3 V. Gutmann, *Coord. Chem. Rev.*, 1976, **18**, 225–255.

4 M. A. Beckett, G. C. Strickland, J. R. Holland and K. S. Varma, *Polymer*, 1996, **37**, 4629–4631.

5 Bruker-AXS, SAINT version 2013.9, 2013, Bruker-AXS, Madison, WI 53711 USA.

6 Bruker-AXS, SADABS version 2012.1, **2012**, Bruker-AXS, Madison, WI 53711, USA.

7 G. M. Sheldrick, *Acta Cryst.*, 2015, **A71**, 3–8.

8 G. M. Sheldrick, *Acta Cryst.*, 2015, **C71**, 3–8.

9 A. L. Spek, *Acta Cryst.*, 2015, **C71**, 9–18.

10 M. J. Frisch, G. W. Trucks, H. B. Schlegel, G. E. Scuseria, M. A. Robb, J. R. Cheeseman, G. Scalmani, V. Barone, G. A. Petersson, H. Nakatsuji, X. Li, M. Caricato, A. V. Marenich, J. Bloino, B. G. Janesko, R. Gomperts, B. Mennucci, H. P. Hratchian, J. V. Ortiz, A. F. Izmaylov, J. L. Sonnenberg, D. Williams-Young, F. Ding, F. Lipparini, F. Egidi, J. Goings, B. Peng, A. Petrone, T. Henderson, D. Ranasinghe, V. G. Zakrzewski, J. Gao, N. Rega, G. Zheng, W. Liang, M. Hada, M. Ehara, K. Toyota, R. Fukuda, J. Hasegawa, M. Ishida, T. Nakajima, Y. Honda, O. Kitao, H. Nakai, T. Vreven, K. Throssell, J. A. Montgomery, Jr., J. E. Peralta, F. Ogliaro, M. J. Bearpark, J. J. Heyd, E. N. Brothers, K. N. Kudin, V. N. Staroverov, T. A. Keith, R. Kobayashi, J. Normand, K. Raghavachari, A. P. Rendell, J. C. Burant, S. S. Iyengar, J. Tomasi, M. Cossi, J. M. Millam, M. Klene, C. Adamo, R. Cammi, J. W. Ochterski, R. L. Martin, K. Morokuma, O. Farkas, J. B. Foresman, and D. J. Fox, Gaussian Development Version (Revision I.13), Gaussian, Inc., Wallingford CT, 2016.

11 V. N. Staroverov, G. E. Scuseria, J. Tao and J. P. Perdew, *J. Chem. Phys.*, 2003, **119**, 12129–12137.